Joint Experimental and DFT Study of the Gas-Phase Unimolecular Elimination Kinetic of Methyl Trifluoropyruvate

María M. Tosta,[†] José R. Mora,[†] Tania Córdova,[‡] and Gabriel Chuchani*[,†]

Centro de Química, Instituto Venezolano de Investigaciones Científicas (IVIC), Apartado 21827, Caracas 1020A, Venezuela, Department of Medicinal Chemistry, College of Pharmacy, University of Florida, P.O. Box 100485, Gainesville, Florida 32610, and Universidad Central, Caracas 1020, Venezuela

Received: May 10, 2010; Revised Manuscript Received: June 15, 2010

The elimination kinetics of methyl trifluoropyruvate in the gas phase was determined in a static system, where the reaction vessel was always deactivated with allyl bromide, and in the presence of at least a 3-fold excess of the free-radical chain inhibitor toluene. The working temperature range was 388.5−430.1 °C, and the pressure range was 38.6−65.8 Torr. The reaction was found to be homogeneous and unimolecular and to obey a first-order rate law. The products of the reaction are methyl trifluoroacetate and CO gas. The Arrhenius equation of this elimination was found to be as follows: log k_1 (s^{-1}) = (12.48 ± 0.32) − (204.2 ± 4.2) kJ $mol^{-1}(2.303RT)^{-1}$ (r = 0.9994). The theoretical calculation of the kinetic and thermodynamic parameters and the mechanism of this reaction were carried out at the B3LYP/6-31G(d,p), B3LYP/6-31++G(d,p), MPW1PW91/6-31G(d,p), MPW1PW91/6-31++G(d,p), PBEPBE/6-31G(d,p), and PBEPBE/6-31G++(d,p) levels of theory. The theoretical study showed that the preferred reaction channel is a 1,2-migration of OCH_3 involving a three-membered cyclic transition state in the rate-determining step.

1. Introduction

The elimination kinetics of ethyl esters of 2-oxocarboxylic acids with nitrogen attached at the acid side, that is, ethyl oxamate and ethyl oxanilinate,[1] suggests that the first step of the reaction is a decarbonylation process by migration of the amino substituent. Similarly, the gas-phase decomposition of ethyl glyoxylate was shown to undergo a parallel and consecutive homogeneous elimination as described in reaction 1,[2] where step 2 is also thought to comprise a decarbonylation followed by H migration.

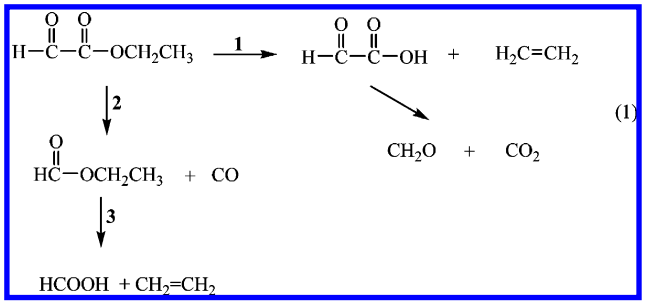

(1)

These mechanistic considerations were derived from experimental and theoretical studies on the gas-phase elimination kinetics of methyl oxalyl chloride.[3] According to this work, a concerted semipolar-type transition state was believed to occur (reaction 2), where the Cl atom migrates to the adjacent carbonyl group as CO gas is eliminated. Semiempirical PM3 and MP2/6-31G* calculations were found to be in good agreement with experiments.

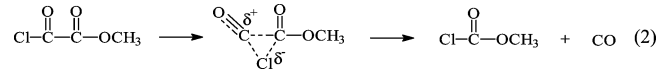

(2)

An apparent interpretation from the above-reported investigations (reaction 2) is that an electron-withdrawing substituent attached at the acid side of the 2-oxo-ester is liable to migrate to the adjacent carbonyl as CO gas is eliminated. Even if a hydrogen atom is included in this consideration (reaction 1, path 2), the result should not be surprising, as Taft's polar substituent constant σ^* of H was defined with a value of +0.49,[4] suggesting a weak electron-withdrawing effect. The few examples reported in the literature are not sufficient to establish a reasonable generalization of the migration phenomenon. It is important to consider the degree of polarization between the substituent at the acid side and the carbon of the C=O. Therefore, the present work was designed to study the CF_3 substituent, which is strongly electron-withdrawing but weakly polarizable, at the 2-oxo-ester. Consequently, the homogeneous, gas-phase elimination kinetics of methyl trifluoropyruvate ($F_3CCOCOOCH_3$) in combination with theoretical calculations was examined. To avoid parallel and consecutive elimination processes, the CH_3 group is preferred at the alkyl side of the 2-oxo-ester.

2. Experimental Method

Methyl trifluoropyruvate (Aldrich) was distilled several times until the fraction had a purity of greater than 99%. The purity of the substrates and products and their identifications were determined by gas chromatography/mass spectrometry (GC/MS) (Saturn 2000, Varian). Capillary column DB-5MS, 30 mm × 0.250 mm i.d. × 0.25 μm, was used. The substrate was quantitatively analyzed by GC (Varian Star 3600 CX) with a thermal conductivity detector (column DB5, 30-m length and 0.53-mm i.d., helium gas carrier).

Kinetics. The experiments were carried out in a static system,[5−7] and the reaction vessel was at all times deactivated

* To whom correspondence should be addressed. E-mail: chuchani@ivic.gob.ve.
[†] Instituto Venezolano de Investigaciones Científicas (I.V.I.C.).
[‡] University of Florida and Universidad Central de Venezuela.

10.1021/jp104238a
Published on Web 07/09/2010

by the product of allyl bromide decomposition. The kinetic measurements were followed manometrically. The temperature was controlled by a Shinko DC-PS resistance thermometer controller, maintained ±0.2 °C, and measured with iron−constantan attached to a Digital Omega 3465B multimeter. Different points along the reaction vessel showed no temperature gradient. The pyruvate, dissolved in chlorobenzene (0.54 M), was injected directly into the reaction vessel with a syringe through a silicon rubber septum. The amount of substrate used for each reaction was ∼0.02−0.1 mL.

3. Computational Method and Model

Theoretical calculations on the kinetics and mechanisms for the gas-phase elimination reaction of methyl trifluoropyruvate were carried out using density functional theory (DFT) with Becke's three-parameter formulation from functional Lee, Yang, and Parr [B3LYP/6-31G(d,p), B3LYP/6-31++G(d,p)]:[8−10] the Perdew−Wang 1991 correlation functional [MPW1PW91/6-31G(d,p), MPW1PW91/6-31++G(d,p)];[11] and the Perdew, Burke, and Ernserhof [PBE/6-31G(d,p), PBE/6-31++G(d,p)][12] methods, as implemented in Gaussian 03.[13]

The default options for convergence in the Berny analytical gradient optimization routines were used; that is, convergence on the density matrix was 10^{-9} atomic units, the threshold value for maximum displacement was 0.0018 Å, and the maximum force was 0.00045 hartree/Bohr. Stationary points, minimum-energy states, and transition states were verified using frequency calculations. Transition state (TS) structures were located using the quadratic synchronous transit (QST) protocol. The TS structures were identified by means of normal-mode analysis by having a single imaginary frequency and the corresponding transition vector (TV). Intrinsic reaction coordinate (IRC) calculations were performed to confirm that the transition state structures connected the reactant and products along the minimum-energy path.

Thermodynamic quantities such as zero-point vibrational energy (ZPVE), temperature corrections [$E(T)$], and absolute entropies [$S(T)$] were obtained from frequency calculations. Temperature corrections and absolute entropies were obtained assuming ideal gas behavior from the harmonic frequencies and moments of inertia by standard methods[14] at average temperature and pressure values within the experimental range. Scaling factors for frequencies and zero-point energies were taken from the literature.[15,16]

The first-order rate coefficient, $k(T)$, was calculated using transition state theory (TST)[17] and assuming that the transmission coefficient is equal to 1, as expressed in the equation

$$k(T) = (k_B T/h) \exp(-\Delta G^{\ddagger}/RT)$$

where $\Delta G^{\ddagger}$ is the Gibbs free energy change between the reactant and the transition state and k_B and h are the Boltzmann and Planck constants, respectively.

$\Delta G^{\ddagger}$ was calculated using the following relations

$$\Delta G^{\ddagger} = \Delta H^{\ddagger} - T\Delta S^{\ddagger}$$

and

$$\Delta H^{\ddagger} = V^{\ddagger} + \Delta\mathrm{ZPVE} + \Delta E(T)$$

TABLE 1: Ratio of Final (P_f) to Initial (P_0) Pressure of the Substrate Methyl Trifluoropyruvate

temp (°C)	P_0 (Torr)	P_f (Torr)	P_f/P_0[a]
398.6	41.4	82.0	2.0
408.8	51.6	99.1	1.9
420.4	57.0	112.5	2.0
430.1	55.1	109.1	2.0

[a] Average = 2.0.

TABLE 2: Stoichiometry of the Reaction[a]

time (min)	reaction (%) (pressure)	substrate decomposition (%) (GC)
8.6	34.2	37.0
20.2	59.8	61.2
23.3	67.8	66.8
27	70.8	74.3
34	79.1	79.4

[a] Substrate = methyl trifluoropyruvate, temperature = 408.5 °C.

TABLE 3: Homogeneity of the Reaction[a]

	$10^4\ k_1$ (s^{-1})	
S/V (cm^{-1})[b]	clean Pyrex vessel	vessel seasoned with allyl bromide
1	24.76 ± 5.01	12.45 ± 0.44
6	59.90 ± 9.56	12.49 ± 0.55

[a] Substrate = methyl trifluoropyruvate, temperature = 420.4 °C. [b] S = surface area (cm^2), V = volume (cm^3).

where $V^{\ddagger}$ is the potential energy barrier and ΔZPVE and $\Delta E(T)$ are the differences in ZPVEs and temperature corrections, respectively, between the TS and the reactant. Entropy values were estimated from vibrational analysis.

4. Results and Discussion

4.1. Experimental Results. The gas-phase elimination of methyl trifluoropyruvate (reaction 3), in vessels deactivated with the product of decomposition of allyl bromide, was found to produce methyl trifluoroacetate and CO gas.

$$F_3CCOCOOCH_3 \rightarrow F_3CCOOCH_3 + CO \qquad (3)$$

The stoichiometry of reaction 3 demands $P_f = 2P_0$, where P_f and P_0 are the final and initial pressures, respectively. The average experimental result for P_f/P_0 at four different temperatures and 10 half-lives was 2.0 (Table 1). An additional verification of the stoichiometry in reaction (3), up to 80% reaction progress, is that the percentage decomposition of the substrate calculated from pressure measurements was in good agreement with the chromatographic analyses of the unreacted pyruvate (Table 2).

The homogeneity of the reaction was tested by using a vessel with a surface-to-volume ratio 6.0 times greater than that of the unpacked vessel (Table 3). The packed and unpacked clean Pyrex vessels had a very significant heterogeneous effect on the substrate. However, when the vessels were seasoned with allyl bromide, no significant effect of the rate coefficients on elimination of the methyl trifluoropyruvate was obtained.

The effect of the addition of different proportions of toluene, a free-radical inhibitor, is described in Table 4. The experiments on the pyruvate were always carried out in seasoned vessels and in the presence of at least 3 times the amount of toluene in

TABLE 4: Effect of the Inhibitor Toluene on the Rate[a]

P_s[b] (Torr)	P_i[c] (Torr)	P_i/P_s	$10^4\ k_1$ (s^{-1})
60	–	–	18.73 ± 5.01
63	65	1.0	17.81 ± 4.16
42	86	2.1	14.12 ± 4.01
52	176	3.4	12.45 ± 0.44
48	206	4.3	12.43 ± 0.40

[a] Substrate = methyl trifluoropyruvate, temperature = 420.2 °C. Vessel seasoned with allyl bromide. [b] P_s = pressure of the substrate. [c] P_i = pressure of the inhibitor.

TABLE 5: Invariability of the Rate Coefficient with the Initial Pressure[a]

P_0 (Torr)	$10^4\ k_1$ (s^{-1})
38.6	11.93 ± 0.41
47.0	11.67 ± 0.55
56.0	11.49 ± 0.27
65.8	11.57 ± 0.72

[a] Substrate = methyl trifluoropyruvate, temperature = 420.2 °C. Vessel seasoned with allyl bromide. In the presence of the inhibitor toluene.

TABLE 6: Temperature Dependence of the Rate Coefficient[a,b]

temperature (°C)	$10^4\ k_1$ (s^{-1})
388.5	2.31 ± 0.08
398.6	4.16 ± 0.19
408.8	7.32 ± 0.24
420.4	12.45 ± 0.44
430.1	20.40 ± 0.82

[a] Substrate = methyl trifluoropyruvate. [b] Rate equation: log k_1 (s^{-1}) = (12.48 ± 0.32) − (204.2 ± 4.2) kJ mol^{-1}(2.303RT)$^{-1}$; r = 0.9994.

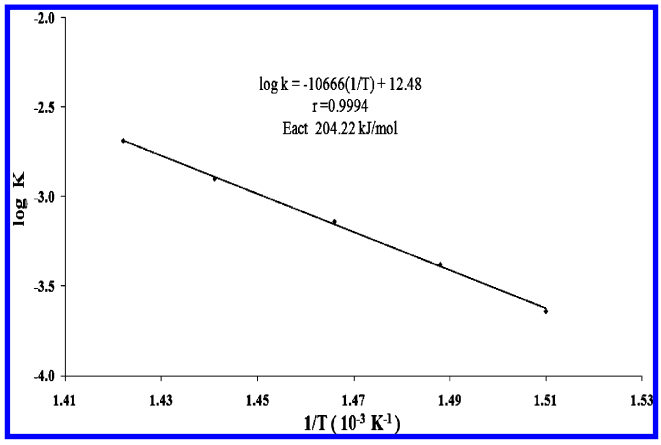

Figure 1. Arrhenius plot for the elimination kinetic of methyl trifluoropyruvate in the gas phase.

order to suppress any possible free-radical chain reaction. No induction period was observed, and the rates were reproducible with a relative standard deviation not greater than 5% at a given temperature.

The first-order rate coefficients of this reaction calculated from $k_1 = -(2.303/t)\ \log[(2P_0 - P_t)/P_0$ were found to be independent of the initial pressures (Table 5). The logarithmic plot of $\log(2P_0 - P_t)$ against time t gave a good straight line up to 75% extent of reaction. The temperature dependence of the rate coefficients and the corresponding Arrhenius equation are given in Table 6 and Figure 1 (90% confidence coefficient obtained from the least-squares procedure).

The results given in Table 6 lead to the consideration of two possible mechanisms for the elimination of methyl trifluoropyruvate as described in reactions 4 and 5. In this respect, a theoretical study was carried out to elucidate which is the most probable and reasonable mechanism according to the experimental data.

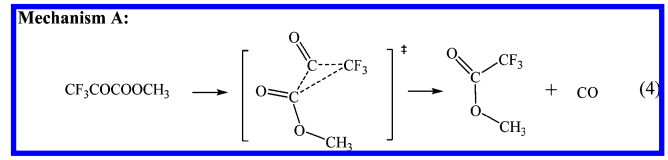

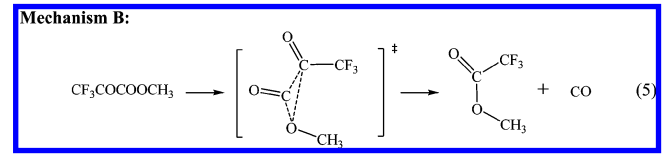

4.2. Theoretical Results. ***4.2.1. Kinetic and Thermodynamic Parameters.*** Theoretical calculations were performed in order to consider a reasonable mechanism for the gas-phase decarbonylation of methyl trifluoropyruvate. Two possible mechanisms were examined, as depicted in reactions 4 and 5. Mechanism A shown in reaction 4 implies the migration of CF_3 to the neighboring carbonyl carbon with loss of CO. Conversely, mechanism B shown in reaction 5 implies the migration of OCH_3 with loss of CO. Both processes proceed in concerted fashion and account for the products formed, methyl trifluoroacetate and carbon monoxide.

Thermodynamic quantities obtained from frequency calculations and the estimated activation parameters were compared with the experimental values. Calculated parameters are given in Table 7. Temperature corrections were carried out at the average experimental conditions (T = 410 °C).

For mechanism A, the calculated enthalpies of activation and energies of activation were overestimated by all DFT methods used by 34−87 kJ/mol when compared to the experimental value. Deviations were also found for the entropy of activation and free energy of activation.

Interestingly, theoretical calculations gave reasonable enthalpies of activation and energies of activation for mechanism B, particularly when using B3LYP/6-31G++(d,p), MPW1PW91/6-31G(d,p), and MPW1PW91/6-31++G(d,p). We found that the PBEPBE method gave underestimated parameters when compared to the experimental values. Regarding the entropy of activation, better results were obtained using MPW1PW91/6-31G(d,p), MPW1PW91/6-31++G(d,p), PBEPBE/6-31G(d,p), and PBEPBE/6-31++G(d,p). However, in considering all calculated parameters, the best agreement with experimental values was obtained with the MPW1PW91 functional. The entropy of activation of about −20 J/(mol K) implies a loss of degrees of freedom corresponding to cyclic transition state structures.

The calculation results are in agreement with mechanism B, suggesting that the gas-phase decarbonylation of methyl trifluoropyruvate is likely to proceed by this reaction channel involving the 1,2-migration of the OCH_3 group to the next carbonyl carbon.

Characterization of the TS structure and a detailed description of the changes in geometrical parameters, charges, and bond orders for mechanism B are provided in the following sections.

4.2.2. Transition State and Mechanism. The optimized structures for reactants, TSs, and products of the reactions

TABLE 7: Thermodynamic and Arrhenius Parameters of Methyl Trifluoropyruvate ($CF_3COCOOCH_3$) at 410 °C

method	E_a (kJ/mol)	log A (s^{-1})	$\Delta H^{\ddagger}$ (kJ/mol)	$\Delta S^{\ddagger}$ [J/(mol K)]	$\Delta G^{\ddagger}$ (kJ/mol)
		Mechanism A			
experimental	204.22	12.48	198.5	−21.2	213.0
B3LYP/6-31G(d,p)	278.8	13.9	273.2	6.8	268.5
B3LYP/6-31++G(d,p)	269.4	13.8	263.7	3.9	261.1
MPW1PW91/6-31G(d,p)	291.2	13.6	285.5	−0.9	285.6
MPW1PW91/6-31++G(d,p)	282.6	13.5	277.0	−1.1	277.7
PBEPBE/6-31G(d,p)	246.0	13.4	240.4	−4.0	243.1
PBEPBE/6-31++G(d,p)	237.6	13.3	231.9	−6.2	236.1
		Mechanism B			
B3LYP/6-31G(d,p)	197.9	13.0	192.2	−12.2	200.6
B3LYP/6-31++G(d,p)	205.6	12.8	199.9	−15.7	210.7
MPW1PW91/6-31G(d,p)	206.7	12.6	201.1	−19.7	214.5
MPW1PW91/6-31++G(d,p)	209.1	12.5	203.4	−20.6	217.5
PBEPBE/6-31G(d,p)	168.1	12.5	162.4	−21.4	177.0
PBEPBE/6-31++G(d,p)	172.7	12.5	167.0	−21.5	181.7

involved in mechanisms A and B are shown in Figures 2 and 3, respectively. The structures of the transition state in the decarbonylation of trifluoropyruvate proceeding through a 1,2-migration correspond to a cyclic three-membered ring. In mechanism A, the migrant group is CF_3, whereas in mechanism B, the migrating group is OCH_3, where the lone pair of electrons on the O atom in OCH_3 moves toward C_2. Because a reasonably good agreement was found between the calculated parameters (Table 7) and the experimental values for mechanism B, in contrast with large deviations found for mechanism A, the data for the geometrical parameters, charges, and bond orders for mechanism B are presented. The atom numbering is shown in Scheme 1.

Interatomic distances reported in Table 8 show a significant elongation of the C_3-O_4 bond in the transition state from 1.33 to 1.85 Å, indicating significant bond breaking. Also, the O_4-C_2 distance decreases considerably from 2.38 to 1.67 Å as the methoxy group migrates from C_3 to C_2. However, the formation of CO is not yet apparent, as indicated by the small change in the C_2-C_3 distance in the TS. The transition vector is associated with a rocking vibration showing the migration of OCH_3 from C_3 to C_2

SCHEME 1

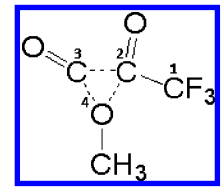

The TS of mechanism B described above was verified by means of IRC calculations. The corresponding plot is given as Supporting Information (Figure 4). To better describe the changes occurring in the proposed reaction channel, further analysis of NBO charges and bond indexes was carried out. The results are discussed in the next two sections.

4.2.3. NBO Charge Analysis. NBO charges have been used to describe the changes in electron distribution occurring in a reaction. Table 9 lists the NBO charges for the relevant atoms

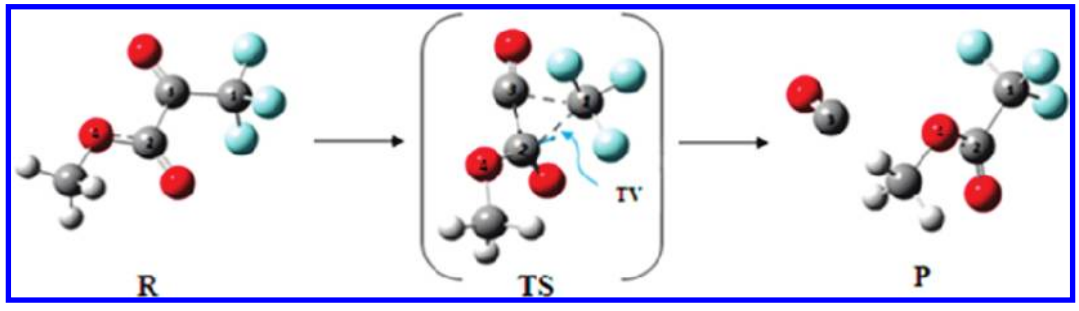

Figure 2. Optimized structures for reactant R, transition state TS, and products P in the gas-phase elimination of $CF_3COCOOCH_3$ at the B3LYP/6-31++G(d,p) level. Mechanism A.

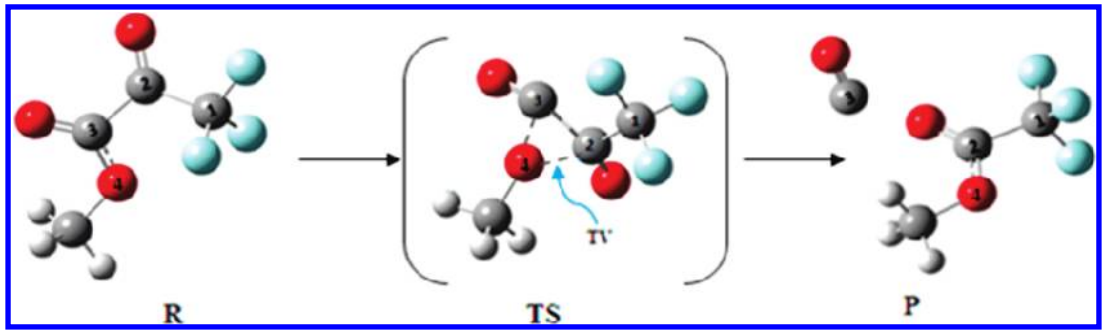

Figure 3. Optimized structures for reactant R, transition state TS, and products P in the gas-phase elimination of $CF_3COCOOCH_3$ at the B3LYP/6-31++G(d,p) level. Mechanism B.

TABLE 8: Structural Parameters of Reactant (R), Transition State (TS), and Products (P) of Methyl Trifluoropyruvate, in Gas-Phase Elimination at 410 °C, Obtained from B3LYP/6-31++G(d,p) Calculations

	Interatomic Distances (Å)		
	C_2-C_3	C_3-O_4	O_4-C_2
R	1.547	1.335	2.380
TS	1.567	1.847	1.669
P	4.457	4.499	1.329
	Angles (deg)		
	$C_2-C_3-O_4$	$C_3-O_4-C_2$	$O_4-C_2-C_3$
TS	57.86	52.65	69.49
	Imaginary Frequency (cm^{-1})		
TS		473.83	

TABLE 9: NBO Charges of Reactant (R), Transition State (TS) and Products (P) of Methyl Trifluoropyruvate, in Gas-Phase Elimination at 410 °C, Obtained from B3LYP/6-31++G(d,p) Calculations

	C_2	C_3	O_4
R	0.416	0.733	−0.533
TS	0.415	0.760	−0.583
P	0.733	0.509	−0.527

of the reactant, TS, and products in the decarbonylation reaction of methyl trifuoropyruvate. Atom numbers are given in Scheme 1.

Calculated NBO charges for the atoms involved in the reaction show augmentation of the negative charge at oxygen O_4 from −0.53 to −0.58 in the TS as the O_4-C_3 bond breaks, accompanied by an increase in the positive charge at carbon C_3 from 0.73 to 0.76. The charge at C_2 is practically unaltered.

The electron distribution in the TS (Table 9) implies the polarization of the O_4-C_3 bond, suggesting that the TS is reactant-like.

4.2.4. Bond Order Analysis. The changes along the reaction coordinates can be studied using NBO bond order calculations.[18−20] For this purpose, Wiberg bond indexes[21] were computed using the natural bond orbital (NBO) program[22] as implemented in Gaussian 03. These indexes can be used to estimate bond orders from population analysis. The bond breaking and making process involved in the reaction mechanism are described by means of the synchronicity (Sy) concept proposed by Moyano et al.,[23] defined by the expression

$$\mathrm{Sy} = 1 - \left[\sum_{i=1}^{n} |\delta B_i - \delta B_{\mathrm{av}}| / \delta B_{\mathrm{av}}\right]/(2n - 2)$$

n is the number of bonds directly involved in the reaction, and the relative variation of the bond index is obtained from

$$\delta B_i = (B_i^{\mathrm{TS}} - B_i^{\mathrm{R}})/(B_i^{\mathrm{P}} - B_i^{\mathrm{R}})$$

where the superscripts R, TS, and P represent the reactant, transition state, and products, respectively.

The evolution in bond change is calculated as

$$E_{\mathrm{v}}\,(\%) = \delta B_i \times 100$$

and the average value is calculated from

$$\delta B_{\mathrm{av}} = \frac{1}{n}\sum_{i=1}^{n} \delta B_i$$

Wiberg bonds indexes, B_i, were calculated for those bonds involved in the changes in the methyl trifluoropyruvate decarbonylation reaction: C_2-C_3, C_3-O_4, and O_4-C_2. (See Table 10.) Other reaction coordinates undergo negligible changes and were not considered.

Calculated parameters show that the single bond order C_3-O_4 was changed from 1.01 to 0.39 in the TS. This coordinate is the most advanced at 63%. Formation of the new single bond O_4-C_2 has an intermediate progress of 47%, whereas breaking of C_2-C_3 shows very little advancement of 8.5%. The synchronicity parameter has been used to describe whether a reaction occurring in a concerted fashion shows equal progress along the different reaction coordinates or not. This parameter varies from 1, in the case of concerted synchronic reaction, to 0 in the case of asynchronous process. Although global synchronicity is a general concept, analysis of bond order in the different reaction coordinates describe the extension to which any particular bond involved in the reaction is formed or broken in the TS. In this sense, the reaction can be described as more advanced in some reaction coordinates than others.

For the elimination of carbon monoxide from methyl trifluoropyruvate, the analysis of bond orders given as Wiberg indexes showed that the process is dominated by the breaking of C_3-O_4 (63%) compared to the other reaction coordinates, and as a result, the reaction is considered asynchronous to a significant extent (Sy = 0.61).

5. Conclusions

The gas-phase decarbonylation reaction of methyl trifuoropyruvate has been studied in a static system with reactor walls deactivated with pyrolysis products with allyl bromide and in the presence of the free-radical inhibitor toluene. The reaction was found to be homogeneous and unimolecular and to obey a first-order rate law. The reaction products are methyl trifluoroacetate and carbon monoxide. The Arrhenius equation of this elimination was found to be $\log k_1\ (s^{-1}) = (12.48 \pm 0.32) - (204.2 \pm 4.2)$ kJ $mol^{-1}(2.303RT)^{-1}$ ($r = 0.9994$). Two mechanisms were studied to account for product formation. Mechanism A proposes CF_3 1,2-migration through a three-membered cyclic transition state, and mechanism B engages OCH_3 1,2-migration also through a cyclic three-membered transition state structure. Theoretical calculations of the potential energy surface encompassing the reactant and products were carried out using different DFT levels with the aim of proposing a reasonable reaction mechanism. The results are in good agreement with the experimental values for migration of a methoxy group rather than a trifluoromethyl group. Comparison of the calculated parameters with experimental values indicates that better results were obtained when using the MPW1PW91 functional and including diffuse functions in the basis set. The suggested

TABLE 10: Wiberg Bond Indexes of Reactant (R), Transition State (TS), and Products (P) of Methyl Trifluoropyruvate, in Gas-Phase Elimination at 410 °C, Obtained from B3LYP/6-31++G(d,p) Calculations

	C_2-C_3	C_3-O_4	O_4-C_2	Sy
B_i^{R}	0.9027	1.0717	0.0179	0.605
B_i^{TS}	0.8264	0.3941	0.5245	
B_i^{P}	0.0004	0.0004	1.0867	
$E_{\mathrm{v}}(\%)$	8.5	63.3	47.4	

reaction channel for this reaction thereby involves OCH_3 1,2-migration. These results imply that, in this type of gas-phase reaction, the OCH_3 group has a better migratory aptitude than the CF_3 group.

Acknowledgment. T.C. is grateful to the Consejo de Desarrollo Científico y Humanístico of Universidad Central de Venezuela (C.D.C.H.) for Grant PG-03-00-6499-2006.

Supporting Information Available: Plot of the IRC describing the energy profile versus the reaction coordinate of the reactant, TS, and products. This information is available free of charge via Internet at http://pubs.acs.org.

References and Notes

(1) Chacin, E. V.; Tosta, M.; Herize, A.; Dominguez, R. M.; Alvarado, Y.; Chuchani, G. *J. Phys. Org. Chem.* **2005**, *18*, 539–545.

(2) Reyes, A.; Dominguez, R. M.; Tosta, M.; Herize, A.; Chuchani, G. *Int. J. Chem. Kinet.* **2007**, *39*, 268–275.

(3) Cordova, T.; Rotinov, A.; Chuchani, G. *J. Phys. Org. Chem.* **2004**, *17*, 148–151.

(4) Hansch, C.; Leo, A. J. *Substituent Constants for Correlation Analysis in Chemistry and Biology*; Wiley: New York, 1979.

(5) Maccoll, A. *J. Chem. Soc.* **1955**, 965–973.

(6) Swinbourne, E. S. *Aust. J. Chem.* **1958**, *11*, 314–330.

(7) Dominguez, R. M.; Herize, A.; Rotinov, A.; Alvarez-Aular, A.; Visbal, G.; Chuchani, G. *J. Phys. Org. Chem.* **2004**, *17*, 399–408.

(8) Becke, A. D. *Phys. Rev. A* **1988**, *38*, 3098.

(9) Becke, A. D. *J. Chem. Phys.* **1993**, *98*, 1372.

(10) Becke, A. D. *J. Chem. Phys.* **1993**, *98*, 5648.

(11) Perdew, J. P.; Wang, Y *Phys. Rev. B* **1992**, *45*, 13244.

(12) Perdew, J. P.; Burke, K; Ernserhof, M. *Phys. Rev. Lett.* **1996**, *77*, 3865–3868.

(13) Frisch, M. J.; Trucks, G. W.; Schlegel, H. B.; Scuseria, G. E.; Robb, M. A.; Cheeseman, J. R.; Montgomery, J. A., Jr.; Vreven, T.; Kudin, K. N.; Burant, J. C.; Millam, J. M.; Iyengar, S. S.; Tomasi, J.; Barone, V.; Mennucci, B.; Cossi, M.; Scalmani, G.; Rega, N.; Petersson, G. A.; Nakatsuji, H.; Hada, M.; Ehara, M.; Toyota, K.; Fukuda, R.; Hasegawa, J.; Ishida, M.; Nakajima, T.; Honda, Y.; Kitao, O.; Nakai, H.; Klene, M.; Li, X.; Knox, J. E.; Hratchian, H. P.; Cross, J. B.; Bakken, V.; Adamo, C.; Jaramillo, J.; Gomperts, R.; Stratmann, R. E.; Yazyev, O.; Austin, A. J.; Cammi, R.; Pomelli, C.; Ochterski, J. W.; Ayala, P. Y.; Morokuma, K.; Voth, G. A.; Salvador, P.; Dannenberg, J. J.; Zakrzewski, V. G.; Dapprich, S.; Daniels, A. D.; Strain, M. C.; Farkas, O.; Malick, D. K.; Rabuck, A. D.; Raghavachari, K.; Foresman, J. B.; Ortiz, J. V.; Cui, Q.; Baboul, A. G.; Clifford, S.; Cioslowski, J.; Stefanov, B. B.; Liu, G.; Liashenko, A.; Piskorz, P.; Komaromi, I.; Martin, R. L.; Fox, D. J.; Keith, T.; Al-Laham, M. A.; Peng, C. Y.; Nanayakkara, A.; Challacombe, M.; Gill, P. M. W.; Johnson, B.; Chen, W.; Wong, M. W.; Gonzalez, C.; Pople, J. A. *Gaussian 03*, revision C.02; Gaussian, Inc.: Wallingford, CT, 2004.

(14) McQuarrie, D. *Statistical Mechanics*; Harper & Row: New York, 1986.

(15) Foresman, J. B., Frish, Æ. *Exploring Chemistry with Electronic Methods*, 2nd ed.; Gaussian, Inc: Pittsburgh, PA, 1996.

(16) (a) Scale factors obtained from Precomputed vibrational scaling factors. *Computational Chemistry Comparison and Benchmark DataBase*; NIST Standard Reference Database 101; National Institute of Standards and Technology (NIST): Gaithersburg, MD; http://cccbdb.nist.gov/vibscalejust.asp. (b) Zheng, J.; Alecu, I. M.; Lynch, B. J.; Zhao, Y.; Truhlar, D. G. Database of Frequency Scaling Factors for Electronic Structure Methods. Minnesota Computational Chemistry, University of Minnesota: Minneapolis, MN; http://comp.chem.umn.edu/truhlar/freq_scale.htm.

(17) Benson, S. W. *The Foundations of Chemical Kinetics*; McGraw-Hill: New York, 1960.

(18) Lendvay, G *J. Phys. Chem.* **1989**, *93*, 4422–4429.

(19) Reed, A. E.; Weinstock, R. B.; Weinhold, F. *J. Chem. Phys.* **1985**, *83* (2), 735–746.

(20) Reed, A. E.; Curtiss, L. A.; Weinhold, F. *Chem. Rev.* **1988**, *88*, 899–926.

(21) Wiberg, K. B. *Tetrahedron* **1968**, *24*, 1083–1095.

(22) Glendening, E. D.; Reed, A. E.; Carpenter, J. E.; Weinhold, F. *Gaussian NBO*, version 3.1; copyright 1995-04, Gaussian, Inc.: Pittsburgh, PA.

(23) Moyano, A; Pericás, M. A.; Valenti, E. *J. Org. Chem.* **1989**, *54*, 573–582.

JP104238A